

Overview

We are analysing the Antarctic Circumpolar Current (ACC) as it is represented in the current AOGCMs. The model data we use are from the World Climate Research Programme's (WCRP's) Coupled Model Intercomparison Project phase 3 (CMIP3) database that was used for the IPCC Fourth Assessment report.

As is known from previous studies (Fyfe and Saenko, 2005, Russell et al., 2006) the ACC strength varies strongly across the CMIP3 models. Our analysis suggests that in addition there is no clear picture about the future changes of the ACC.

In order to find the reason for this discrepancy we are trying to analyse exactly how the ACC is balanced in the models. This involves the zonal momentum balance on the one hand and the meridional density gradient on the other hand.

The CMIP3 models

The data used here are the last 20 years of the control runs and the years 2081-2099 of the SRES A1B scenario, from all models that provided the 3D ocean fields*. Model numbers used in this poster's figures are given below.

model	model
1 bccr_bcm2_0	14 ingv_echam4
2 cccma_cgcm3_1_t47	15 inmcm3_0
3 cccma_cgcm3_1_t63	16 ipsl_cm4
4 cnrm_cm3	17 miroc3_2_hires
5 csiro_mk3_0	18 miroc3_2_medres
6 csiro_mk3_5	19 miub_echo_g
7 gfdl_cm2_0	20 mpi_echam5
8 gfdl_cm2_1	21 mri_cgcm2_3_2a
9 giss_aom	22 ncar_ccsm3_0
10 giss_eh_2	23 ncar_pcm1
11 giss_model_e_h	24 ukmo_hadcm3
12 giss_model_e_r	25 ukmo_hadgem1
13 iap_fgoals1_0_g	26 observed

* The GFDL and MPI data were partly obtained separately.

Zonal momentum

There is a significant linear relation between the ACC strength and the maximum zonal wind stress (Fig. 1) if a few outlier models are disregarded.

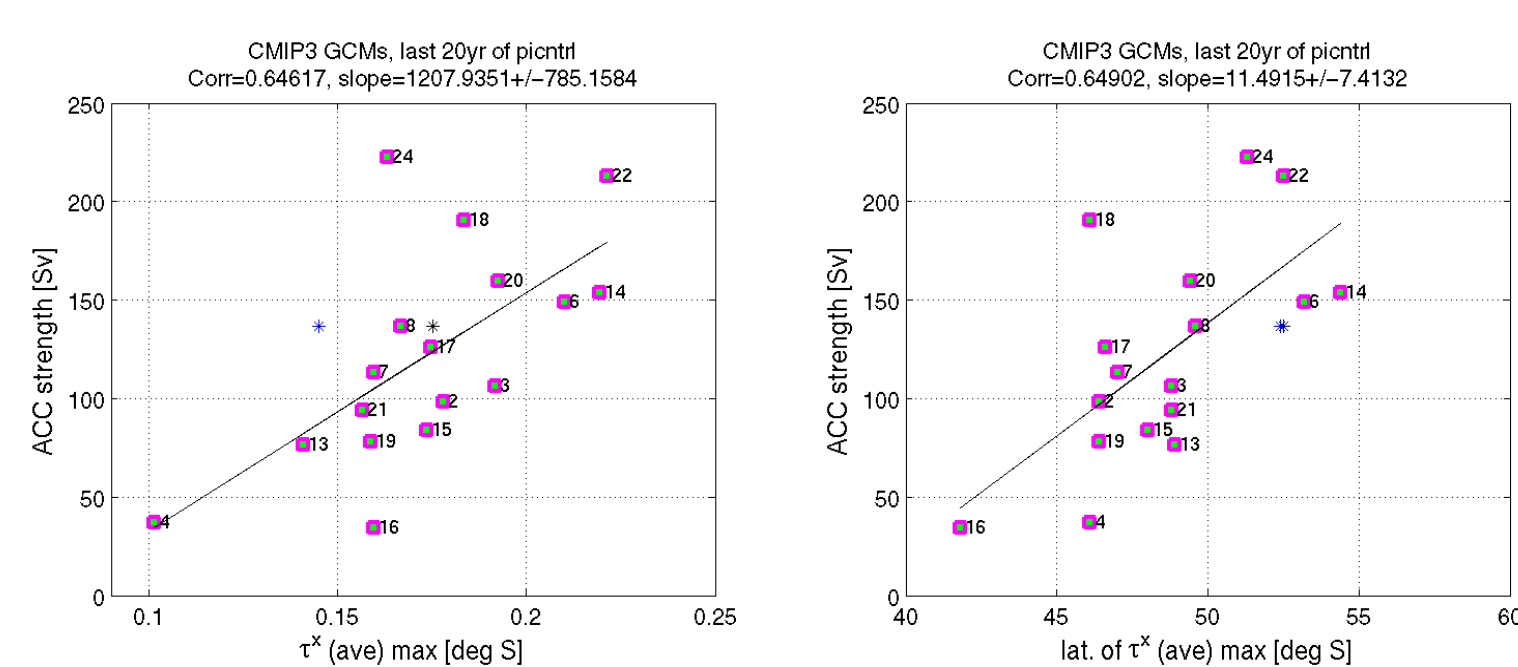


Figure 1. ACC strength (averaged, in Sv) versus the maximum wind stress (left) and the position of the maximum (right). The dashed line shows the linear fit. Each dot represents one model; their numbers are given in the table above. Asterisks indicate observations: SCOW (blue; 1999-2007) and ERA-15 (1978-1994, black).

Theoretically the surface wind stress, τ_x , should be balanced by bottom form stress since friction, τ_f , is expected to be small (as are the lateral fluxes; Hughes and de Cuevas 2001, Vallis 2009):

$$\tau_x = \tau_f - \int H \cdot \frac{\partial p_b}{\partial x} dx \quad (1)$$

For HadCM3 this is true (the bottom friction is zero) and we are in the process of analysing the other models. Note that (1) is zonally and vertically integrated. The zonal velocity is not contained and the ACC is involved only indirectly through the bottom pressure p_b .

ACC change in the end of the 21st century

We compared the ACC strength in the models' control runs with the projected strength in the end of the 21st century in the SRES A1B scenario (Fig. 2).

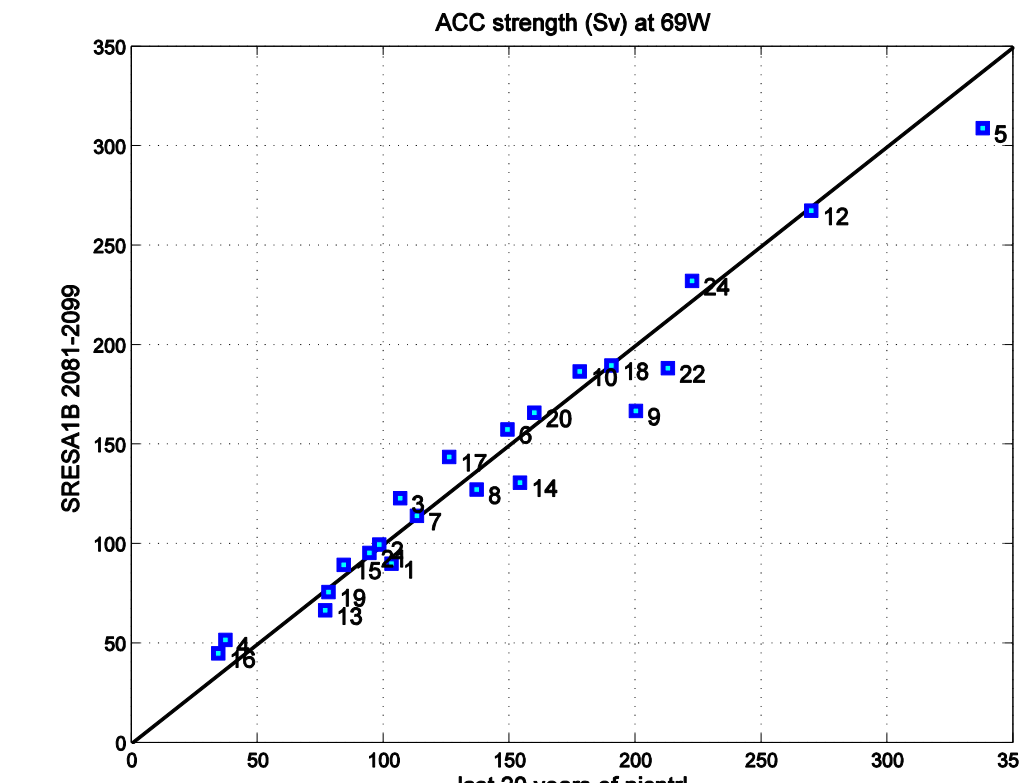


Figure 2. ACC strength (averaged, in Sv) in the control run (x-axis) and the SRES A1B scenario (y-axis). Each dot represents one model whose numbers are given in the table below. The black line is the line of no change. Models above that line show an increase of the ACC in the A1B scenario.

The mean ACC across the models is 146 +/- 72 Sv in the control run and 142 +/- 68 Sv in the SRES A1B scenario. While there is a drop in the mean value, this is obscured by the inter-model variability. In observations from the period 1993-2000 no change can be detected (Cunningham et al., 2003).

Across the CMIP3 models the relative change of the ACC in the SRES A1B scenario varies greatly (Fig. 3).

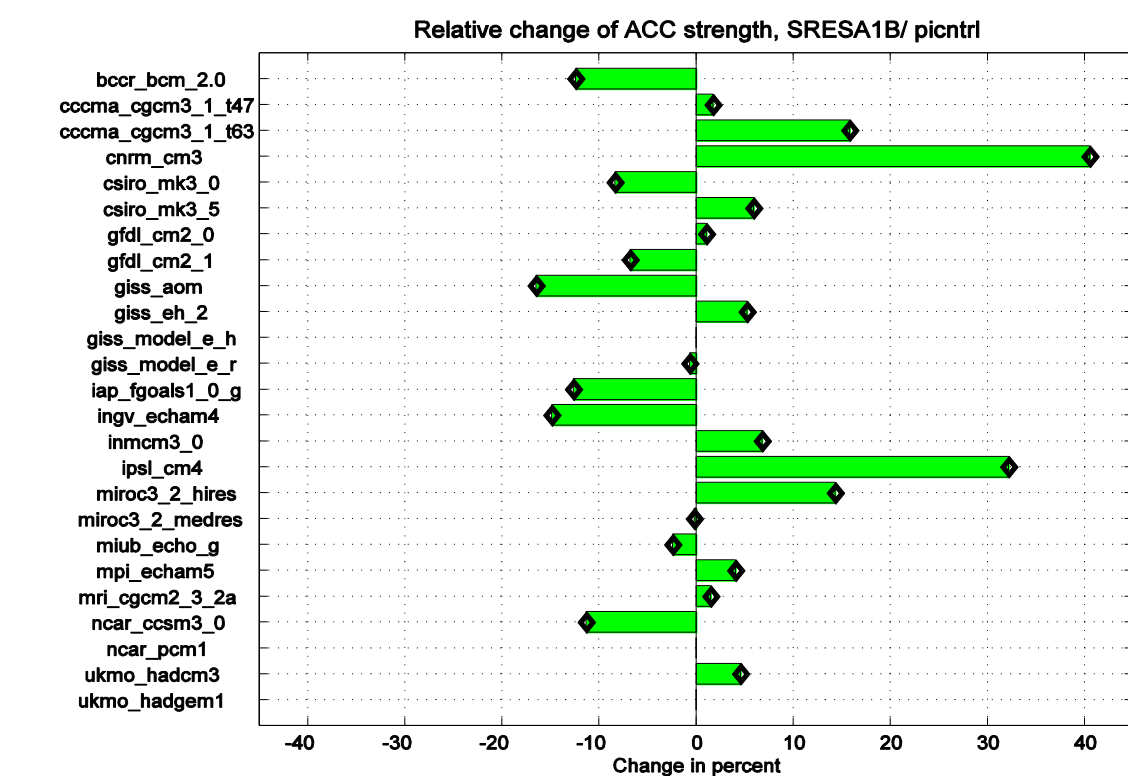


Figure 3. Changes of the ACC in percent, SRES A1B 2081-2099 averaged, relative to the last 20 years of control run averaged. No value is given for a model if either or both of the values were unavailable.

There is no discernible trend even though all models do show a strengthening of the wind stress maximum and a polar shift (or at least no shift; not shown). In contrast to these results, Fyfe and Saenko (2005) did find indications for a stronger ACC in the future. However, we use here different scenarios, more models and a different ACC diagnostic.

ACC strength and AABW

There is a significant linear relation between the AABW volume transport at 30°N in the Atlantic and the ACC strength (Fig. 4). This might be due to denser AABW leading to a stronger meridional density gradient across the ACC and to a stronger AABW inflow.

This led us to look for a reliable diagnostic of AABW formation in the Southern Ocean.

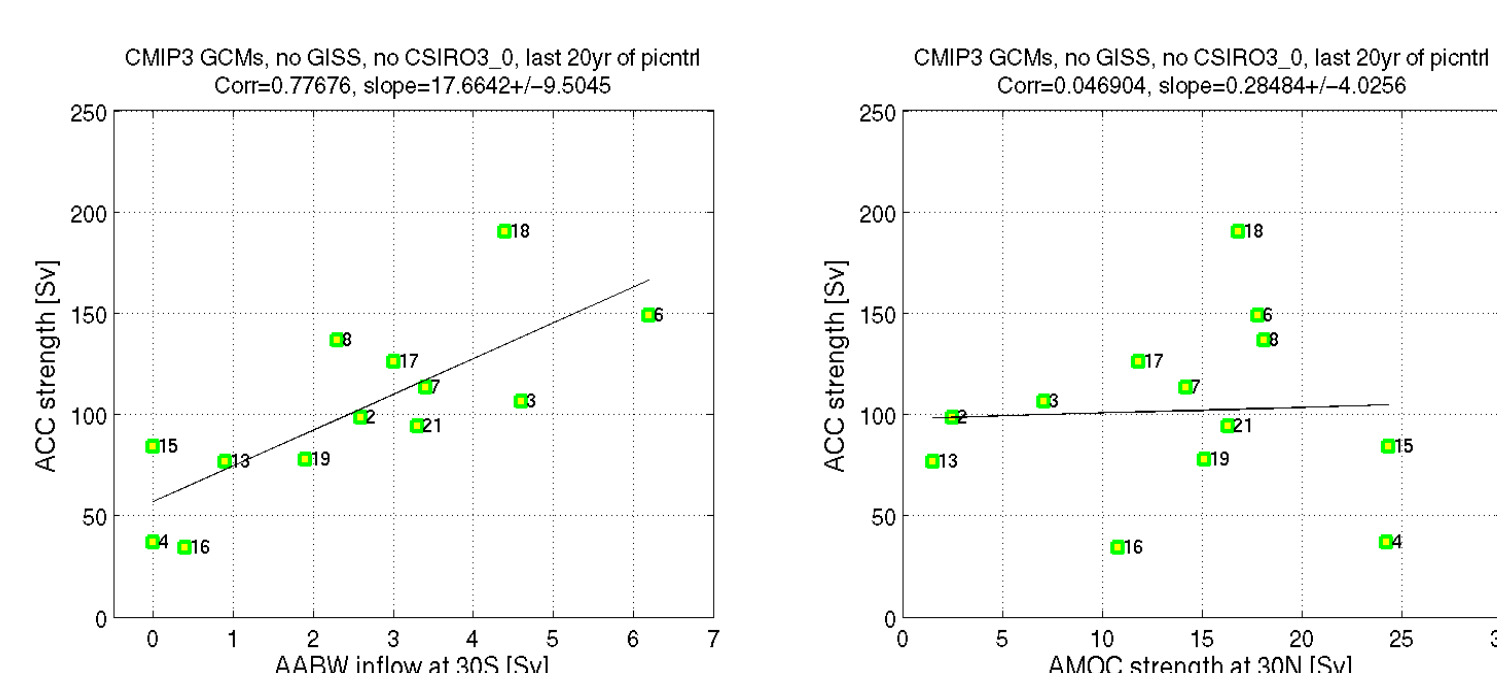


Figure 4. Left: Transport of AABW into the Atlantic at 30°S, diagnosed from the meridional streamfunction, versus the ACC strength (averaged, in Sv). Right: maximum AMOC strength at 30N versus the ACC strength. Significant correlations between the ACC and the AMOC could not be found.

Isopycnal streamfunction

The meridional streamfunction on depth levels tends to misrepresent the circulation in the Southern Ocean due to the Deacon cell. We are computing the streamfunction on isopycnal levels instead. The example below (Fig. 5) shows an AABW cell that has a local maximum at about 60°S where it nearly connects to the surface densities.

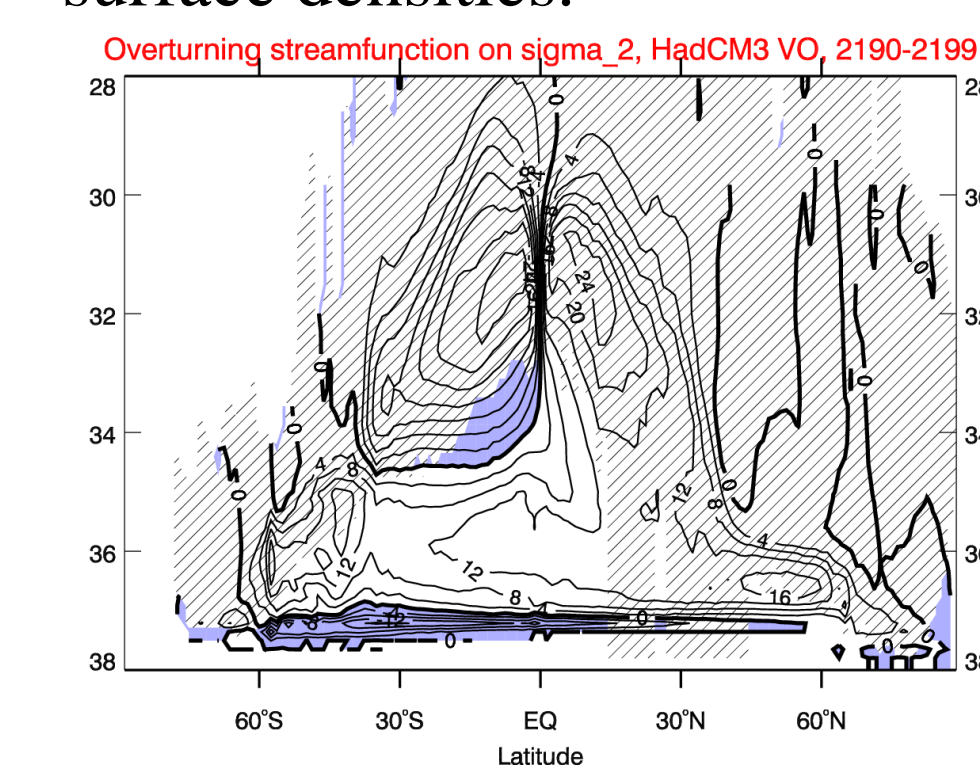


Figure 5. Meridional overturning streamfunction on isopycnals (σ_2), averaged from the last 10 years of the HadCM3 control run using the large-scale velocity VO. White cells indicate clockwise transport, blue cells anti-clockwise. Hatched areas denote the range of surface densities at each latitude.

In most AOGCMs the eddy transports across the ACC are represented by an eddy-induced transport velocity (Gent and McWilliams, 1990). Its streamfunction (Fig. 6, left) affects the water masses through tracer transport.

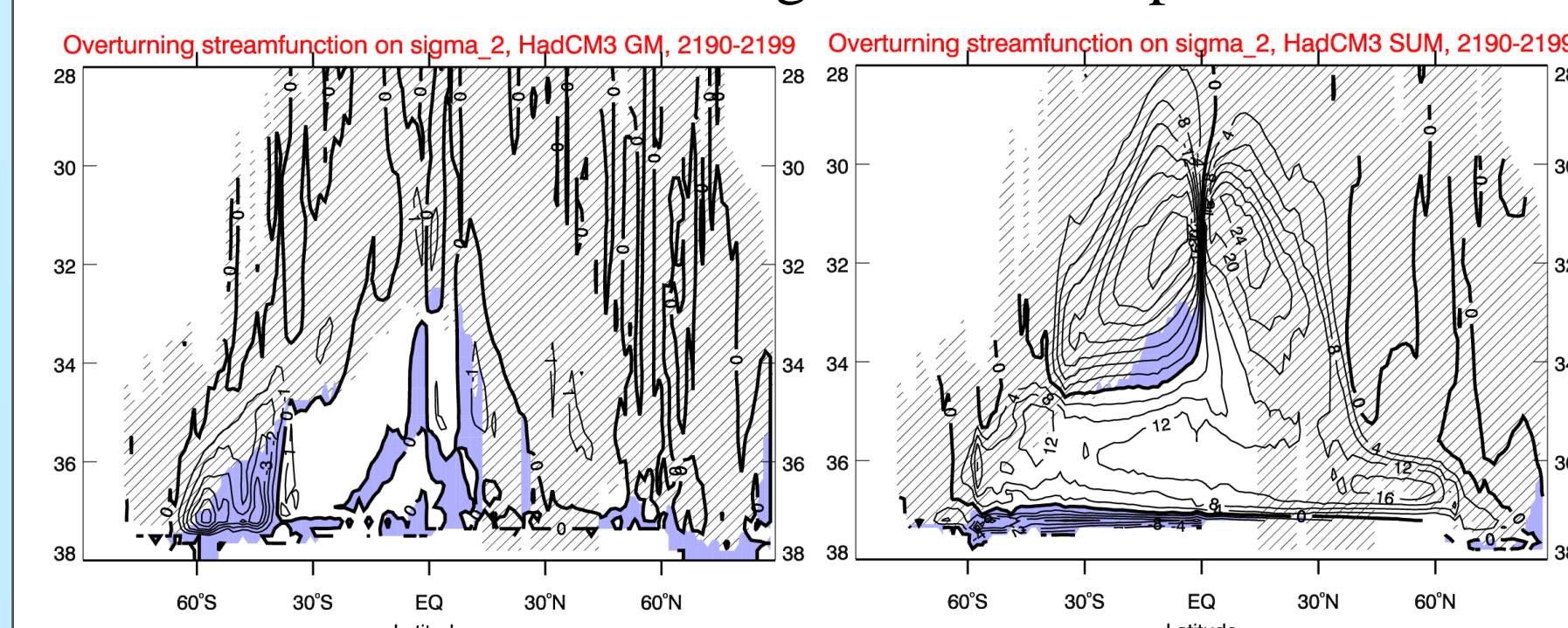


Figure 6. (left) Meridional overturning streamfunction on σ_2 of the GM velocities of HadCM3. Note the cell of 6 Sv at Drake Passage latitudes. (right) Sum of the VO streamfunction (from Fig. 5) and the GM streamfunction.

In further work we will use the isopycnal streamfunction to (1) diagnose the AABW volume transport and (2) inquire the role of the parameterised eddy transports in setting the stratification in the Southern Ocean. Eq. (1) suggests that the wind stress input is balanced by an integral of the full stratification.

Acknowledgments

We acknowledge the modeling groups, the Program for Climate Model Diagnosis and Intercomparison (PCMDI) and the WCRP's Working Group on Coupled Modelling (WGCM) for their roles in making available the WCRP CMIP3 multi-model dataset. Support of this dataset is provided by the Office of Science, U.S. Department of Energy.

We are grateful to Alistair Hind for assistance with the analyses. This research was supported by a Marie Curie Intra-European Fellowship within the 7th European Community Framework Programme.

References

- Cunningham, S. A., S. G. Alderson, B. A. King, and M. A. Brandon, 2003, *J. Geophys. Res.* 108 (C5), 8084
- Fyfe, J. C., and O. A. Saenko, 2005, *GRL* 33, L06701
- Gent, P. R. and J. C. McWilliams, 1990, *JPO* 20, 150-155
- Hughes, C. W., and B. A. de Cuevas, 2001, *JPO* 31, 2871-2885
- Russell, J. L., R. J. Stouffer, and K. W. Dixon, 2006, *J. Clim.* 19, 4560-4575
- Vallis, G. K., 2009, *Atmospheric and Oceanic Fluid Dynamics*. Cambridge University Press

Contact

Till Kuhlbrodt
Department of Meteorology, NCAS-Climate
University of Reading
Earley Gate, Reading RG6 6BB, UK
phone: +44 118 378 6014
t.kuhlbrodt@reading.ac.uk